Electronic Supplementary Material (ESI) for Dalton Transactions.

Supporting Information for

Differences in Chemoselectivity in Olefin Oxidation by a series of Mn^{IV} – oxo Complexes

Priya Singh,[a] Melissa C. Denler,[a] Jaycee R. Mayfield,[a] and Timothy A. Jackson*[a]

[a] *The University of Kansas, Department of Chemistry and Center for Environmentally Beneficial Catalysis, 1567 Irving Hill Road, Lawrence, KS 66045, USA.*

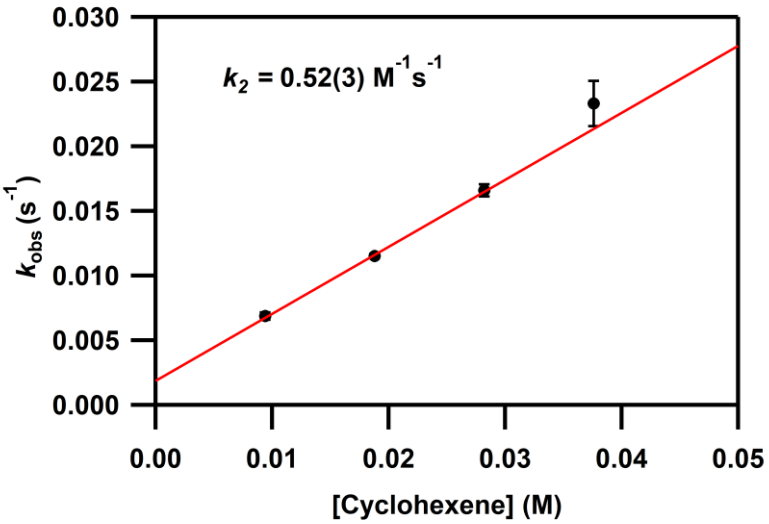

Figure S1. Plot of the pseudo-first-order rate constant (k_{obs}) against substrate concentration for the reaction between $[Mn^{IV}(O)(2pyN2Q)]^{2+}$ (**2**) and cyclohexene in TFE for substrate dissolved in CH_2Cl_2.

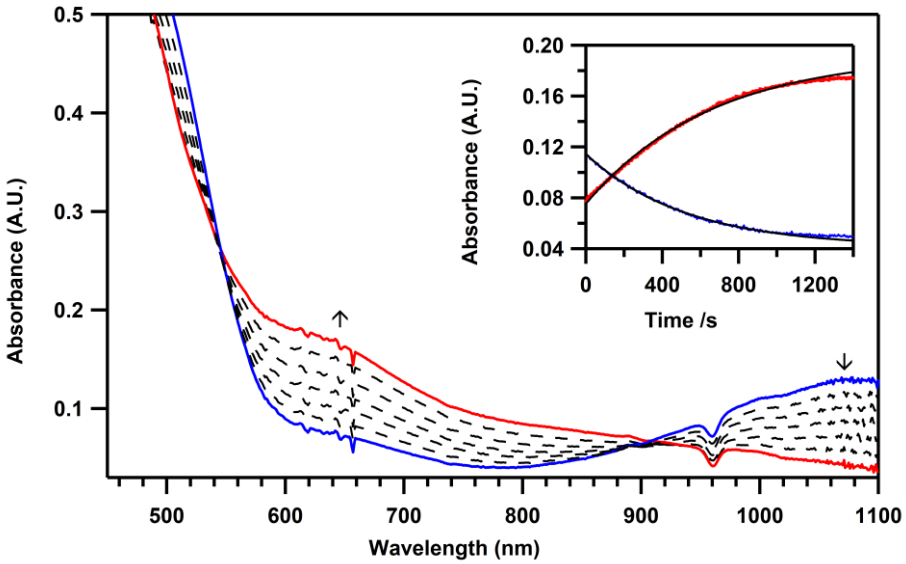

Figure S2. Electronic absorption spectra showing the reaction of 1.0 mM $[Mn^{IV}(O)(2pyN2Q)]^{2+}$ (**2**) with 200 µL MeCN (~1740 equiv.) in TFE at 25 °C. Inset: decay of the feature at 1020 nm (k_{obs} = 1.9(3) x 10^{-3} s^{-1}) and the growth of the feature at 620 nm (k_{obs} = 1.5(2) x 10^{-3} s^{-1}).

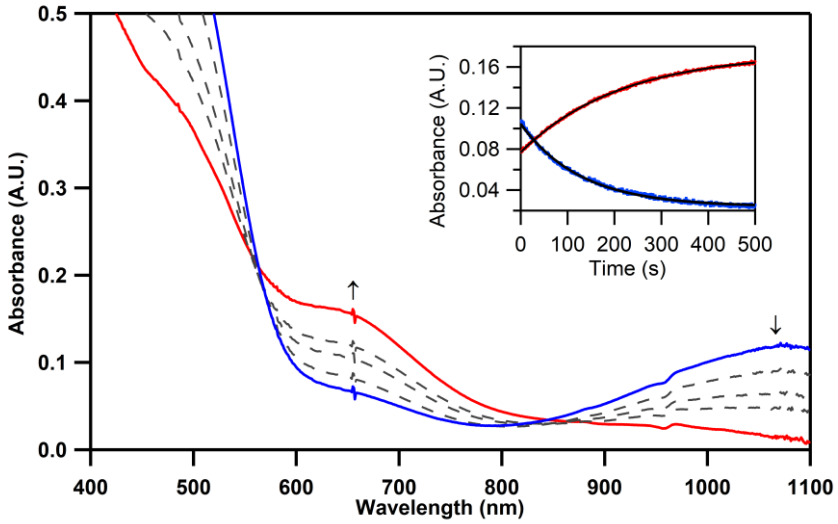

Figure S3. Electronic absorption spectra of reaction of 1.0 mM $[Mn^{IV}(O)(N2py2Q)]^{2+}$ (**2**) with 40 equiv. cylcohexene-d_{10} in TFE. Inset: decay of the feature at 1020 nm (k_{obs} = 7.8(6) × 10^{-3} s^{-1}) and the growth of the feature at 620 nm (k_{obs} = 4.7(2) × 10^{-3} s^{-1}).

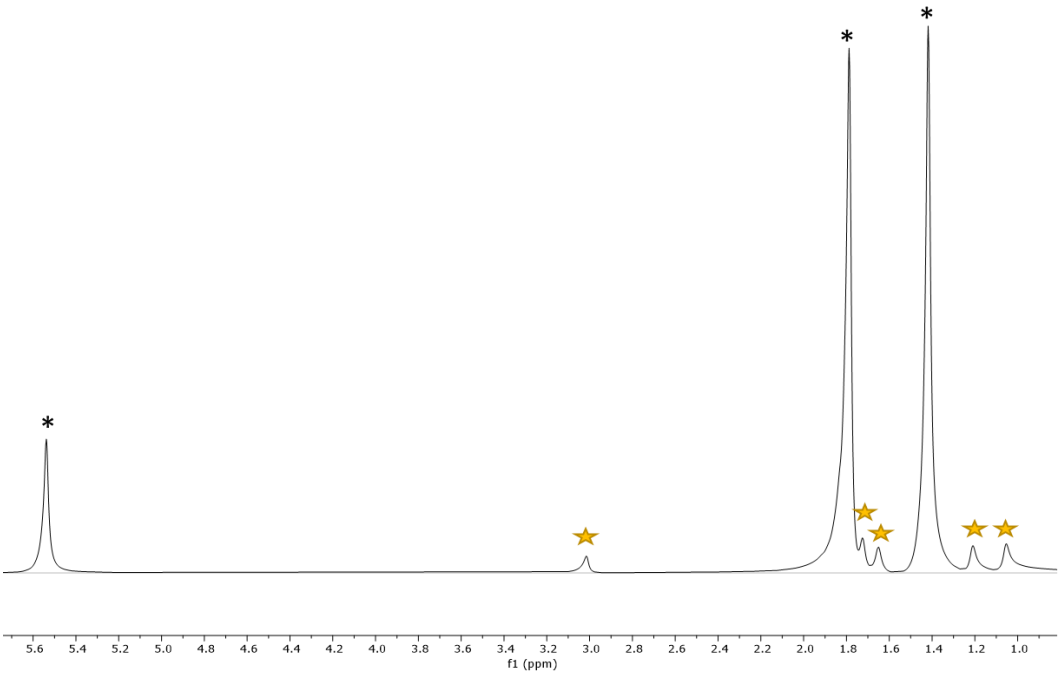

Figure S4. ^{2}H NMR spectrum of the product of the reaction of cyclohexene-d_{10} with $[Mn^{IV}(O)(N2py2Q)]^{2+}$ (**2**) in CF_3CH_2OH/CH_3CN (*v/v* = 19:1) at 298 K. The signals have been referenced to $CDCl_3$. The asterisk indicates excess cyclohexene-d_{10} and the stars indicate cyclohexene oxide-d_{10}.

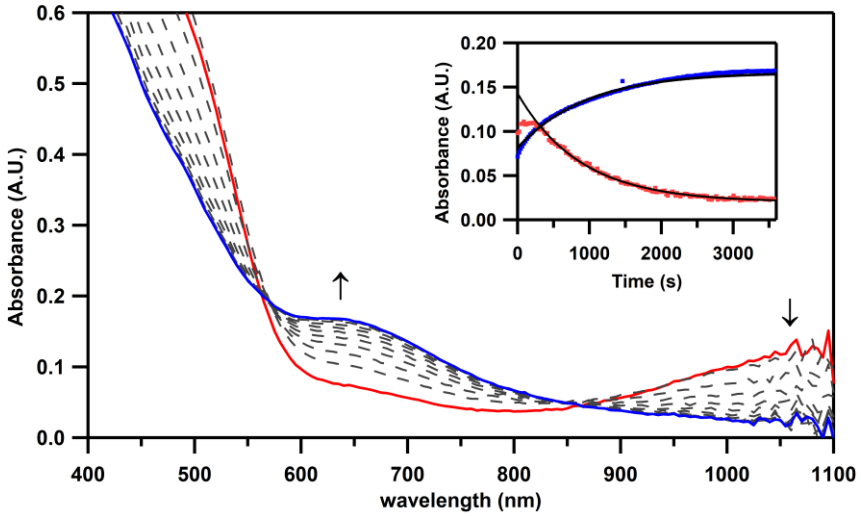

Figure S5. Electronic absorption spectra of the reaction of 1.0 mM $[Mn^{IV}(O)(N2py2Q)]^{2+}$ (**2**) and 1.0 mM $[Mn^{II}(N2py2Q)]^{2+}$ in TFE at 298 K. Inset: decay of the feature at 1020 nm (k_{obs} = 1.1(2) × 10^{-3} s^{-1}) and the growth of the feature at 620 nm (k_{obs} = 1.1(3) × 10^{-3} s^{-1}).

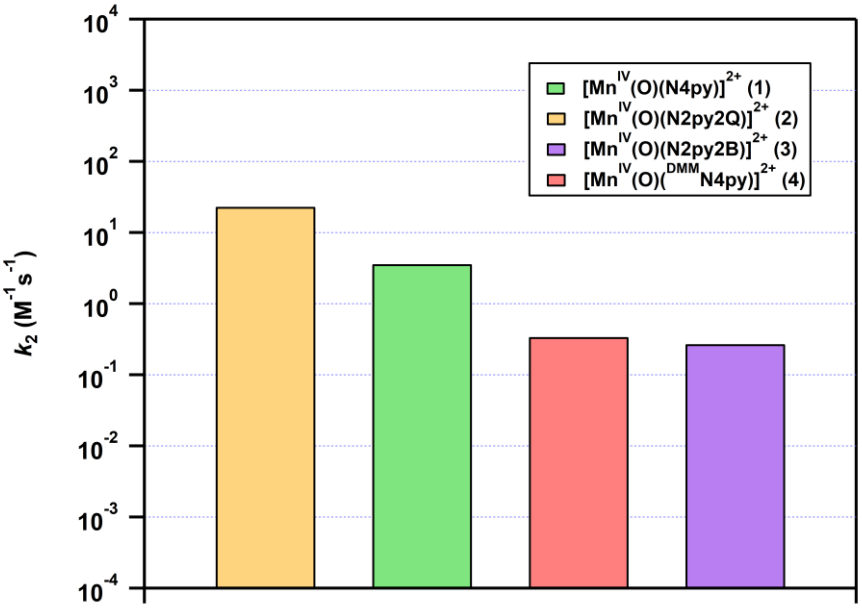

Figure S6. Comparison of second-order rate constants obtained for the reactions of 9,10-dihydroanthracene (DHA) and Mn^{IV} – oxo adducts in TFE at 298 K.

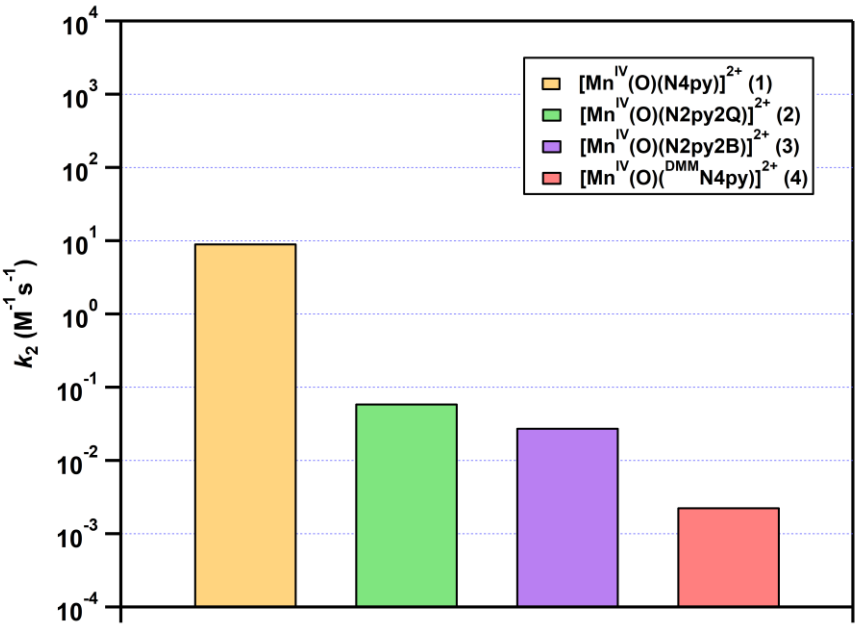

Figure S7. Comparison of second-order rate constants obtained for the reactions of thioanisole and Mn^{IV} – oxo adducts in TFE at 298 K.

Computational details

The Bordwell equation (main article, equation 3) used to calculate $Mn^{III}O-H$ BDFE for **1-4** consist of the term C_G (free energy constant). This term represents the solvent dependence of the BDFE values as both the reduction potential and pK_a terms in the Bordwell equation are highly influenced by the identity of the solvent. Ideally, we would include a C_G value for TFE, which is the solvent used for all the experimental data. However, we are unaware of a C_G value for this solvent. Consequently, while we employed the C_G value for acetonitrile (52.6)[1] to determine absolute BDFEs, we will discuss ΔBDFEs relative to **1**.

The $E_{1/2}$ of $Mn^{IV/III}$ couples was calculated using equation 4 and 5, based on the isodesmic reaction model between Mn^{IV}-oxo complexes and **1** (scheme S1a) where experimental $Mn^{IV/III}$ reduction potential of **1** was used as reference to account for systematic errors. Similarly, experimentally known pK_a of $[Mn^{IV}(OH)_2(Me_2EBC)]^{2+}$ was used as reference to calculate pK_a values of **1-4** for the reaction shown in scheme S1b using the equation 4 and 6. These results have been summarized in Table S1.

$$E_{rxn} = products - reactants \quad \text{... Equation 4}$$

$$E_{1/2,calc}(V) = \frac{E_{rxn,2a}}{23.06\,V} + E_{1/2,exp}(V) \quad \text{... Equation 5}$$

$$pK_{a,calc} = \frac{E_{rxn,2b} + pK_{a,exp}(kcal\,mol^{-1})}{1.37} \quad \text{... Equation 6}$$

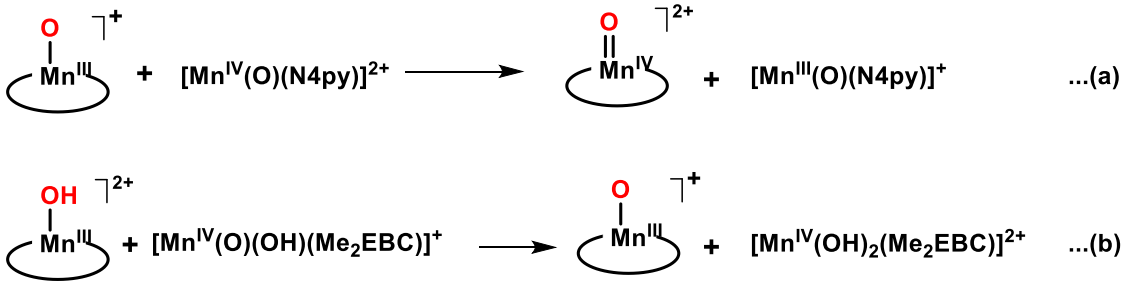

Scheme S1. a) Isodesmic reaction between Mn^{IV}-oxo complexes (**1-4**) and **1** for determination of reduction potential of **1-4**; b) Model reaction for determination of pK_a of **1-4** using $[Mn^{IV}(OH)_2(Me_2EBC)]^{2+}$ reference.

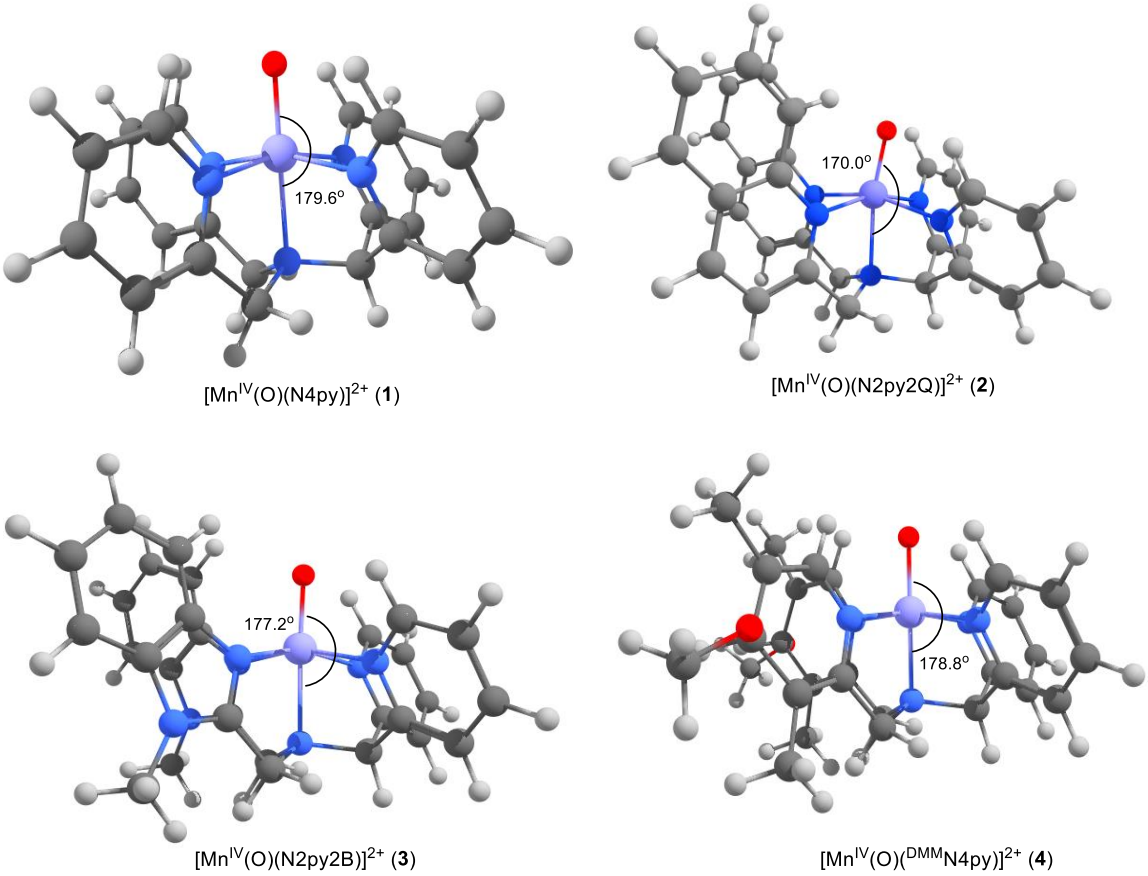

Figure S8. DFT computed structures of Mn^{IV}-oxo complexes **1-4** with axial (N_{ax}-Mn-O) angle distortion displayed.

Table S1. DFT calculated free energy of the reaction between Mn^{IV}-oxo species and dimethyl sulfide (DMS).

Complexes	$[Mn^{IV}(O)(N4py)]^{2+}$ (**1**)	$[Mn^{IV}(O)(N2py2Q)]^{2+}$ (**2**)	$[Mn^{IV}(O)(N2py2B)]^{2+}$ (**3**)	$[Mn^{IV}(O)(^{DMM}N4py)]^{2+}$ (**4**)
ΔG_{DFT}	-19.34	-22.96	-18.86	-14.93

Table S2. DFT calculated values of pK_a, $E_{1/2}$ and $Mn^{III}O-H$ BDFEs.

Complexes	**pK_a**	**$E_{P,C}$**	**ΔBDFE**	**BDFE**
$[Mn^{III}(OH)(N4py)]^{2+}$	18.35	0.80	0.00	98.49
$[Mn^{III}(OH)(N2py2Q)]^{2+}$	17.42	1.05	4.42	102.91
$[Mn^{III}(OH)(^{DMM}N4py)]^{2+}$	18.73	0.71	-1.58	96.91
$[Mn^{III}(OH)(N2py2B)]^{2+}$	20.54	0.55	-2.73	95.75

Table S3. Summary of DFT calculated electronic energies, entropies and free energies of the species discussed in this work.

Complexes	**Electronic Energy kcal/mol**	**Zero Point Energy kcal/mol**	**ΔH^{I}= Electronic + ZPE**	**vib**	**rot**	**trans**	**G**
$[Mn^{IV}(O)(N4py)]^{2+}$ (**1**)	-1498773.64	256.58	-1498517.06	21.53	10.56	13.16	-1498562.31
$[Mn^{IV}(O)(N2py2Q)]^{2+}$ (**2**)	-1691572.90	315.54	-1691257.36	27.34	10.96	13.34	-1691309.00
$[Mn^{IV}(O)(N2py2B)]^{2+}$ (**3**)	-1713226.36	328.09	-1712898.27	30.55	11.00	13.35	-1712953.17
$[Mn^{IV}(O)(^{DMM}N4py)]^{2+}$ (**4**)	-1741171.40	365.81	-1740805.59	36.11	11.10	13.36	-1740866.16
$[Mn^{III}(OH)(N4py)]^{2+}$	-1499327.12	261.81	-1499065.31	23.85	10.6	13.16	-1499112.92
$[Mn^{III}(OH)(N2py2Q)]^{2+}$	-1692124.74	321.01	-1691803.73	29.46	10.99	13.34	-1691857.52
$[Mn^{III}(OH)(N2py2B)]^{2+}$	-1713777.93	333.31	-1713444.62	32.89	11.04	13.35	-1713501.90
$[Mn^{III}(OH)(^{DMM}N4py)]^{2+}$	-1741714.81	369.97	-1741344.84	39.85	11.13	13.37	-1741409.19
$[Mn^{II}(TFE)(N4py)]^{2+}$	-1735747.62	289.68	-1735457.94	31.50	10.92	13.31	-1735513.67
$[Mn^{II}(TFE)(N2py2Q)]^{2+}$	-1928550.81	348.48	-1928202.33	36.95	11.22	13.47	-1928263.97
$[Mn^{II}(TFE)(N2py2B)]^{2+}$	-1950199.97	360.74	-1949839.23	40.08	11.26	13.48	-1949904.05
$[Mn^{II}(TFE)(^{DMM}N4py)]^{2+}$	-1978140.37	398.67	-1977741.70	46.55	11.36	13.49	-1977813.10
TFE	-284134.17	35.83	-284098.34	3.08	7.89	11.84	-284121.15
DMSO	-347117.04	49.53	-347067.51	2.73	7.42	11.62	-347089.28
DMS	-299926.75	47.17	-299879.58	2.11	7.03	11.42	-299900.14

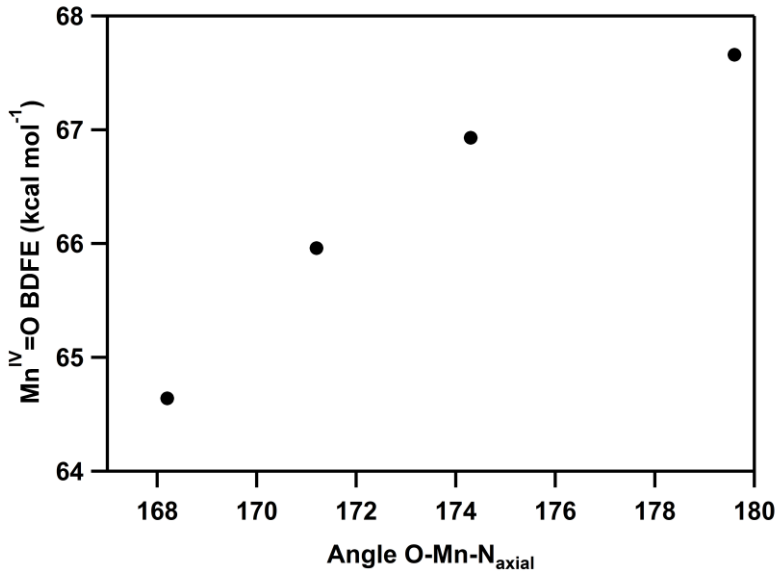

Figure S9. A correlation between Mn^{IV}=O BDFE and distortion of the axial angle (O-Mn-N_{ax}) from ideal value of 180°.

Reference:

1. S. V. Lymar, M. Z. Ertem and D. E. Polyansky, *Dalton Transactions*, 2018, **47**, 15917-15928.